Available online at www.sciencedirect.com
SCIENCE DIRECT®
International Journal of Heat and Mass Transfer 47 (2004) 3003–3015
International Journal of HEAT and MASS TRANSFER
www.elsevier.com/locate/ijhmt

Effect of viscous dissipation on the optimization of the heat transfer in internally finned tubes

Giampietro Fabbri *

Dipartimento di Ingegneria Energetica, Nucleare e del Controllo Ambientale, Universitá degli studi di Bologna, Viale Risorgimento 2, 40136 Bologna, Italy

Received 18 July 2003; received in revised form 5 March 2004

Abstract

In the present work the effect of viscous dissipation on the heat transfer in a finned tube cooled by a fluid in laminar flow is studied under the condition of imposed heat flux. In particular, the alterations induced by viscous dissipation in the optimum finned tube geometries are investigated. To this aim, the velocity and temperature distributions on the finned tube cross-section are determined with the help of a finite element model which takes the effect of viscous dissipation into account. Moreover, a global heat transfer coefficient is calculated. After having assigned a polynomial lateral profile to the fins of the tube, the geometry is then optimized in order to maximize the heat transferred per unit of tube length for a given weight and for a given hydraulic resistance in correspondence with different intensities of viscous dissipation. Lastly, the differences between the optimum geometries obtained under different conditions of viscous dissipation are analyzed.

1. Introduction

In many practical applications the effect of viscous dissipation on the laminar forced convection cannot be neglected. This occurs for example when the dimension of the duct is small or the viscosity of the fluid is high. Compact heat exchangers often are used under these conditions. In fact, to make such devices more and more compact, the fluids are forced to flow inside very small channels. Moreover, to remove the heat from certain motors, the lubricating fluid, which is strongly viscous, is also cooled through a compact heat exchanger, as in case of motor vehicles.

One of the earliest study on the effect of viscous dissipation on laminar forced convection was carried out by Brinkman, who investigated the heat transfer in capillary ducts under both the boundary condition of imposed wall temperature and insulated duct wall [1]. Afterwards, many authors investigated the effect of viscous dissipation on laminar forced convection under different geometrical, physical, and boundary conditions [2–12]. Tyagi [2] studied the effect of viscous dissipation on the heat transfer in the fully developed velocity and temperature profile region of arbitrary cross-section tubes under the condition of uniform wall temperature. The viscous dissipation in the entrance region was analyzed by Ou and Cheng [3,4] under both the condition of temperature or heat flux uniformly imposed on the tube wall. The effects of viscous dissipation under condition of uniform temperature or heat flux were also compared by Basu and Roy [6]. In general, it has been observed that viscous dissipation is more effective when changes in the fluid velocity on the duct cross-section are high. Moreover, in case of fully developed laminar convection and imposed heat flux on the duct wall, viscous dissipation results in a reduction of the Nusselt number.

In a previous work [13], we studied the problem of optimizing the heat transfer in an internally finned cylindrical tube by varying the fin shape under the conditions of laminar flow and imposed heat flux on the tube wall. As in most of the studies on the laminar

* Tel.: +39-51-61-44510; fax: +39-51-61-44516.
E-mail address: giampietro.fabbri@mail.ing.unibo.it (G. Fabbri).

0017-9310/$ - see front matter © 2004 Elsevier Ltd. All rights reserved.
doi:10.1016/j.ijheatmasstransfer.2004.03.007

Nomenclature

a	height of the fins (m)
Br_e	equivalent Brinkman number
c_p	specific heat capacity of the coolant (J/kg K)
f	fin profile angle as a function of r (rad)
E	surface averaging matrix (m^2)
e_{ij}	elements of the surface averaging matrix E (m^2)
h	global heat transfer coefficient (W/m^2 K)
k_c	thermal conductivity of the coolant (W/m K)
n	polynomial order
Nu_e	equivalent Nusselt number
p	generalized pressure (N/m^2)
q''	heat flux per unit of surface (W/m^2)
r	radial coordinate (m)
r_i	radial coordinate of the ith node (m)
R	internal radius (m)
S	vector containing the total area of the four subelements surrounding each node (m^2)
S_p	area of the studied portion of the tube cross-section (m^2)
s	unfinned wall thickness (m)
T	vector containing the temperature of each node (K)
T_b	bulk temperature of the coolant (K)
t	temperature in the solid and in the fluid on the tube cross-section (K)
t_i	temperature of the ith node (K)
T_{max}	maximum temperature on the external surface (K)
U	vector containing the coolant velocity of each node (m/s)
u	coolant velocity (m/s)
$\overline{u}$	average coolant velocity (m/s)
u_i	coolant velocity of the ith node (m/s)
z	longitudinal coordinate (m)

Greek symbols

α	normalized height of the fins
β	angle between two symmetry axes (rad)
γ	ratio between finned tube and coolant thermal conductivity
Δ	vector containing the values of the viscous dissipation function in each node (Pa/s)
δ	viscous dissipation function (Pa/s)
δ_i	viscous dissipation function in the ith node (Pa/s)
ς	normalized hydraulic resistance
η	normalized radial coordinate
θ	angular coordinate (rad)
θ_i	angular coordinate of the ith node (rad)
μ	dynamic viscosity (Pa s)
ξ	normalized area of the fin cross-section
ρ	coolant density (kg/m^3)
σ	normalized unfinned wall thickness
$\overline{\sigma}$	normalized average wall thickness
ϕ	fin profile angle as a function of η (rad)
ϕ_i	fin profile describing parameters
ψ_i	polynomial coefficients

convection in finned cylindrical tubes, the effect of viscous dissipation was neglected. However, the results obtained in our previous study demonstrated that it is possible to noticeably improve the heat transfer effectiveness of finned cylindrical tubes by assigning to the fins a wavy profile. Moreover, the improvements observed in the heat transfer are caused by higher velocity gradients which induce higher temperature gradients and heat fluxes near the surface of the fins [13]. Therefore, such improvements are expected to be reduced by the effect of viscous dissipation.

In the present work we then study the problem of optimizing the geometry of internally finned cylindrical tubes by taking viscous dissipation into consideration. In particular, the heat transfer in an internally finned tube is investigated under the condition of laminar coolant flow, fully developed velocity and temperature profiles, and imposed heat flux on the tube wall (as in counter-current flow heat exchangers). To this aim, a mathematical model is proposed, which considers the thermal phenomena induced by changes in the fin profile as well as viscous dissipation. Moreover, an opportune genetic algorithm [14–17] is utilized in order to find the optimum fin shape under different conditions of viscous dissipation.

2. The finned tube model

Let us consider a tube with internal fins, which are identical and have an axial symmetrical cross-section (Fig. 1a). A heat flux q'', is uniformly imposed on the external surface. Moreover, a coolant passes through the tube in laminar flow.

As in the case viscous dissipation is negligible [13], the heat transfer performances of the system can be determined by studing a portion of it delimited by two symmetry axes (Fig. 1b). Let us choose a cylindrical coordinate system with the z-axis directed as the coolant flow. Let a be the fin height in the radial direction and $f(r)$ an arbitrary function of the radial coordinate r which provides the value of the angular coordinate θ on

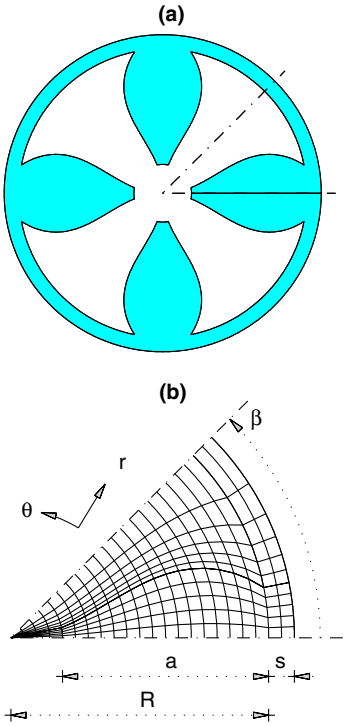

Fig. 1. Finned tube geometry: cross-section (a), subdivision of a portion of the cross-section in finite elements (b).

the lateral fin profile. Moreover, let R the internal radius, s the unfinned tube wall thickness and β the angle between the symmetry axes.

Let us introduce the following hypotheses:

1. the system is in steady state,
2. velocity and temperature profiles are completely developed,
3. fluid properties are uniform,
4. natural convection is negligible in regard to the forced one,
5. viscous dissipation is not negligible.

These hypotheses can be assumed, for example, for a heat exchanger working continuously or for long periods, having tubes whose length is significantly large with respect to the radius, transferring heat fluxes which are not so high to create very large changes in the temperature on the cross-section, and supplied by a fluid flowing at a moderate-high velocity.

The coolant flow is then described by the following equation [18]:

$$\frac{1}{r}\frac{\partial}{\partial r}\left(r\frac{\partial u}{\partial r}\right)+\frac{1}{r^2}\frac{\partial^2 u}{\partial \theta^2}=\frac{1}{\mu}\frac{\mathrm{d}p}{\mathrm{d}z} \tag{1}$$

μ being the dynamic viscosity and p a generalized pressure, which includes the gravitation potential. Eq. (1) must be integrated by imposing the following boundary conditions:

1. on the contact surfaces with the solid the velocity is zero,
2. on the symmetry axes and center the partial derivative of the velocity in the normal direction is zero.

The temperature distribution in the coolant is described by the following equation [18]:

$$\rho c_p u\frac{\partial t}{\partial z}=k_{\mathrm{c}}\left[\frac{1}{r}\frac{\partial}{\partial r}\left(r\frac{\partial t}{\partial r}\right)+\frac{1}{r^2}\frac{\partial^2 t}{\partial \theta^2}\right]+\delta(r,\theta) \tag{2}$$

ρ being the density, c_p the specific heat, and k_{c} the thermal conductivity of the coolant, and δ a viscous dissipation function:

$$\delta(r,\theta)=\mu\left[\left(\frac{\partial u}{\partial r}\right)^2+\frac{1}{r^2}\left(\frac{\partial^2 u}{\partial \theta^2}\right)^2\right] \tag{3}$$

The temperature distribution in the finned tube is instead described by Laplace's equation:

$$\frac{1}{r}\frac{\partial}{\partial r}\left(r\frac{\partial t}{\partial r}\right)+\frac{1}{r^2}\frac{\partial^2 t}{\partial \theta^2}=0 \tag{4}$$

Eqs. (2) and (4) must be integrated by imposing the following boundary conditions:

1. on the contact surface, the temperature is the same in the solid and in the fluid;
2. on the contact surface, the heat flux in the normal direction is the same in the solid and in the fluid;
3. on the symmetry axes and center, the heat fluxes in the normal direction are zero;
4. on the external tube surface, the heat flux in radial direction is equal to $-q''$.

The value of the temperature in one point of the section is also required.

Due to the complexity of the problem, Eqs. (1), (2) and (4) can be integrated numerically. As in Ref. [13], by adequately locating some nodes, the portion of the cross-section of the finned tube can be subdivided in an array of elements delimited by two concentric arches and two segments (Fig. 1b). In the center of the tube an element with the form of a circle sector can be located, supposing that in this element changes in the coolant velocity and temperature are negligible.

Let the velocity vector, the temperature, and the viscous dissipation function in each element of the coolant be approximated by an interpolation of the values which they assume in the four nodes of the element:

$$u(r,\theta)=\sum_i N_i(r,\theta)u_i \tag{5}$$

$$t(r,\theta)=\sum_i N_i(r,\theta)t_i \tag{6}$$

$$\delta(r,\theta)=\sum_i N_i(r,\theta)\delta_i \tag{7}$$

$N(r,\theta)_i$ being form factors:

$$N_i(r,\theta)=\frac{\ln r-\ln r_{j(i)}}{\ln r_i-\ln r_{j(i)}}\,\frac{\theta-\theta_{k(i)}}{\theta_i-\theta_{k(i)}} \tag{8}$$

and r_i, r_j, θ_i, θ_k being node coordinates.

Let us subdivide each element in four subelements by joining the middle points of the opposite sides. By integrating Eq. (1) on the four subelements surrounding each node where the velocity is unknown and Eq. (2) or (4) where the temperature is unknown, the following systems of equations are obtained:

$$A*U=B \tag{9}$$

$$C*T=D \tag{10}$$

where the known vectors B and D are:

$$B=\frac{1}{\mu}\frac{\mathrm{d}p}{\mathrm{d}z}S \tag{11}$$

$$D=\frac{1}{k_c}\left(\rho c_p\frac{\partial t}{\partial z}E*U-q''L-E*\Delta\right)-C_{kn}T_{kn} \tag{12}$$

In Eqs. (9)–(12) vector U and T contain the values of the velocity and temperature, respectively, in the nodes where they are unknown, vector T_{kn} the value of the temperature in the node where it is known, vector S the total area of the four subelements surrounding the nodes, vector L the total perimeter of the four subelements surrounding the nodes crossed by q'', vector Δ the values of the viscous dissipation function, and E is a surface integration matrix. Notice that, to correctly integrate Eqs. (2) and (4) on the four subelements surrounding a node located on the contact surface between fluid and solid, the boundary condition of the same heat flux in the fluid and the solid in the direction normal to the contact surface must be taken into account. Such a condition requires the thermal conductivity of the solid to be considered with respect to that of the fluid. Therefore, some of the elements of matrix C also depend on the ratio γ between the thermal conductivity of the solid and the fluid.

Since properties are uniform and independent of the temperature, system (9) can be solved separately. After solution of system (9), the discrete distribution of the velocity is obtained and the convective and dissipative terms of Eq. (12) can be calculated. Since the derivative of the temperature in the z-direction is still unknown, Eqs. (2) and (4) must be integrated on the whole portion of the tube cross-section S_p, including the finned wall:

$$\rho c_p\frac{\partial t}{\partial z}\int_{S_p}u\,\mathrm{d}s=(R+s)\beta q''+\int_{S_p}\delta\,\mathrm{d}s \tag{13}$$

Referring to the discrete distribution of the velocity, the partial derivative of the temperature in the z-direction then results:

$$\frac{\partial t}{\partial z}=\frac{(R+s)\beta q''+\sum_i\sum_j e_{ij}\delta_j}{\rho c_p\sum_i\sum_j e_{ij}u_j} \tag{14}$$

where e_{ij} are the elements of matrix E and the summation indices i and j are extended to all the nodes of the coolant. Vector D can now be written as follows:

$$D=\frac{1}{k_c}\left[\frac{(R+s)\beta q''+\sum_i\sum_j e_{ij}\delta_j}{\sum_i\sum_j e_{ij}u_j}E*U-q''L-E*\Delta\right]-C_{kn}T_{kn} \tag{15}$$

After solution of system (10) the discrete distribution of the temperature is obtained as a function of T_{kn}.

We can now calculate some parameters in order to evaluate the heat transfer performance of the finned tube. The bulk temperature, a global heat transfer coefficient, and the equivalent Nusselt number can be calculated as in Ref. [13]:

$$T_b=\frac{\sum_i\sum_j e_{ij}u_jt_j}{\sum_i\sum_j e_{ij}u_j} \tag{16}$$

$$h=\frac{q''}{T_{max}-T_b} \tag{17}$$

$$Nu_e=\frac{h2(R+s)}{k_c} \tag{18}$$

where the summation indices i and j are extended to all the nodes of the coolant and T_{max} is the maximum temperature on the external tube wall surface.

The global heat transfer coefficient is calculated by referring to the maximum temperature of the surface on which the heat flux is imposed. In many practical applications, in fact, the heat transfer is limited by the maximum temperature which the materials of the cooled system can support. This is the case of the cooling of an electronic device whose external case temperature cannot exceed the limit prescribed by the producer, or the case of the heat removing from a nuclear fuel rod whose cladding cannot exceed the melding temperature. In these application, the cooling system performing the best is that which is able to remove the highest heat flux for a given drop between the maximum surface temperature and bulk temperature.

The equivalent Nusselt number is calculated referring to the external radius. In this way, it represents the Nusselt number which would be calculated if the same heat flux dissipated by the finned tube were transferred,

under all other conditions, through an unfinned tube having a wall with ideally null thickness and the same external dimension of the finned tube. In many practical applications, in fact, the space which is available for the cooling system is limited and, in particular, the tube performing the best is that which is able to remove the highest heat flux for a given external radius.

The normalized hydraulic resistance ς, moreover, can be calculated as the ratio between the hydraulic resistance of the finned tube and that of an unfinned tube with the same internal radius:

$$\varsigma = \frac{\beta}{2\pi}\frac{(-\mathrm{d}p/\mathrm{d}z)}{\sum_j e_{ij}u_j}\Bigg/\frac{8\mu}{\pi R^4}. \tag{19}$$

Since the system is linear referring to the temperature, an arbitrary value can finally be assigned to T_{kn} in order to calculate the global heat transfer coefficient and the equivalent Nusselt number of the finned tube.

3. Results

In order to investigate the effect of viscous dissipation on the optimum geometry of an internally finned cylindrical tube, the above described mathematical model has been used in the same genetic algorithm of Ref. [13].

Referring to the following dimensionless variable:

$$\alpha = \frac{a}{R}, \quad \eta = \frac{r}{R}, \quad \sigma = \frac{s}{R}, \quad \phi(\eta) = f(\eta R) \tag{20}$$

a polynomial form has been assigned to the profile function ϕ:

$$\phi(\eta) = \sum_{i=0}^{n} \psi_i \eta^i \tag{21}$$

As fin profile describing parameters the values of ϕ in $n+1$ equidistant points on the η-axis has been chosen:

$$\phi_i = \phi\left(1 - \frac{i}{n}\alpha\right) \quad \forall\ i = 0, 1, \ldots, n \tag{22}$$

The genetic algorithm has been used to find the combination of parameters α, β, σ and ϕ_i which allow the maximum Nu_e to be obtained respecting some constraining conditions and in correspondence with different intensities of viscous dissipation.

To ensure the structural integrity of the finned tube, σ has been imposed to be no less than 0.05 and $\phi(\eta)$ to be no less than 0.05β. Moreover, to ensure a uniform distribution of the fluid into the channels between the fins, $\phi(\eta)$ has been imposed to be no greater than 0.95β. Finally, α has been constrained to an established value (0.8), since the genetic algorithm tried to extend the height of the fins as much as possible in order to create separated narrow channels.

To constrain the volume and the weight of the tube wall, the average wall thickness $\overline{\sigma}$ has been considered:

$$\overline{\sigma} = \sqrt{(1+\sigma)^2 + \frac{\xi}{\beta}} - 1 \tag{23}$$

ξ being the area of the fin cross-section:

$$\xi = 2\sum_{i=0}^{n} \psi_i(\phi_0, \ldots, \phi_n)\frac{1-(1-\alpha)^{i+2}}{i+2} \tag{24}$$

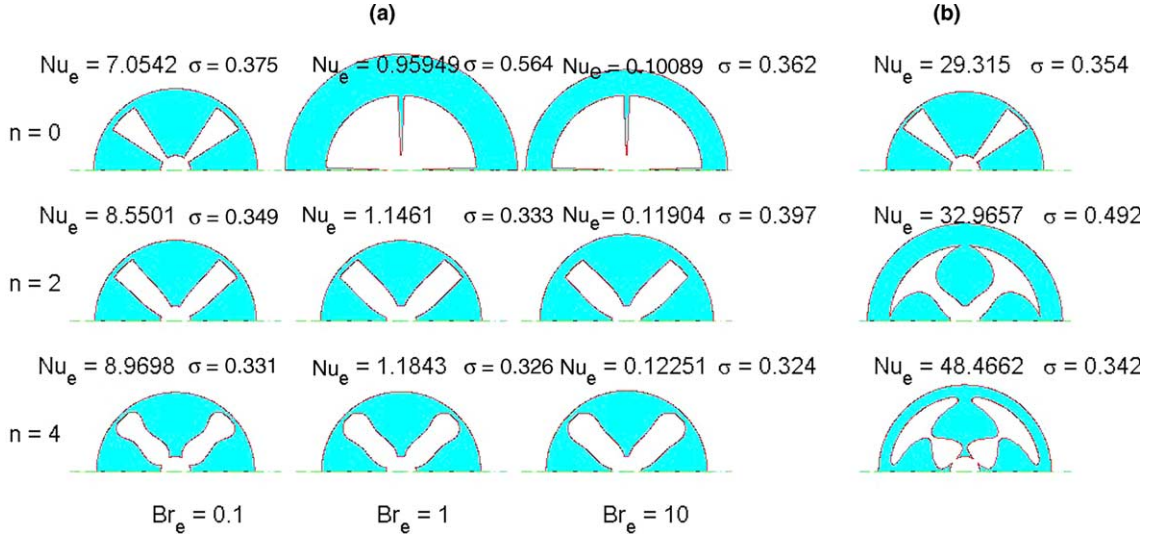

Fig. 2. Finned tube geometries which maximize Nu_e when α is equal to 0.8, β to $\pi/4$ and γ to 500, when the effect of viscous dissipation is considered (a) and neglected (b).

Table 1
Characteristic parameters of some optimum finned tube geometries (cases are listed in the same order they are discussed in the text)

γ	n	Br_e	$\overline{\sigma}$	σ	ϕ_0	ϕ_1	ϕ_2	ϕ_3	ϕ_4	Nu_e	ς	Figure
500	0	0.1	0.375	0.09	0.5756	–	–	–	–	7.054	88.88	2
500	0	1	0.564	0.548	0.0412	–	–	–	–	0.959	5.16	2
500	0	10	0.362	0.344	0.0394	–	–	–	–	0.101	5.14	2
500	2	0.1	0.349	0.074	0.6082	0.5382	0.3097	–	–	8.55	62.67	2
500	2	1	0.333	0.071	0.6114	0.4994	0.2277	–	–	1.146	45.15	2
500	2	10	0.397	0.154	0.6186	0.4858	0.2027	–	–	0.119	41	2
500	4	0.1	0.331	0.052	0.6825	0.5806	0.5826	0.387	0.4379	8.97	67.81	2
500	4	1	0.326	0.06	0.7085	0.5515	0.5354	0.372	0.2445	1.184	46.79	2
500	4	10	0.324	0.073	0.6958	0.5276	0.4926	0.3405	0.1497	0.123	34.93	2
500	0	0.1	0.1	0.05	0.0879	–	–	–	–	6.475	5.93	6
500	0	1	0.1	0.078	0.0393	–	–	–	–	0.958	5.13	6
500	0	10	0.1	0.078	0.0393	–	–	–	–	0.101	5.13	6
500	2	0.1	0.1	0.05	0.1621	0.0606	0.0427	–	–	6.548	5.56	6
500	2	1	0.1	0.05	0.1678	0.0576	0.047	–	–	0.986	5.55	6
500	2	10	0.1	0.05	0.1706	0.0565	0.0493	–	–	0.104	5.55	6
500	4	0.1	0.1	0.05	0.2851	0.0424	0.0768	0.0821	0.0396	6.645	5.67	6
500	4	1	0.1	0.05	0.3107	0.0627	0.0425	0.0462	0.0425	1.005	5.43	6
500	4	10	0.1	0.05	0.3034	0.0645	0.0426	0.0472	0.0406	0.106	5.44	6
500	0	0.1	0.2	0.126	0.14	–	–	–	–	6.528	7.02	7
500	0	1	0.2	0.179	0.041	–	–	–	–	0.959	5.16	7
500	0	10	0.2	0.18	0.0393	–	–	–	–	0.101	5.13	7
500	2	0.1	0.2	0.05	0.3812	0.252	0.0394	–	–	6.986	10.21	7
500	2	1	0.2	0.05	0.582	0.1682	0.0401	–	–	1.065	9.16	7
500	2	10	0.2	0.05	0.5935	0.1634	0.0409	–	–	0.113	9.13	7
500	4	0.1	0.2	0.05	0.3619	0.2053	0.5282	0.2377	0.1877	7.599	19.3	7
500	4	1	0.2	0.05	0.6051	0.3046	0.2016	0.1037	0.0403	1.069	9.31	7
500	4	10	0.2	0.05	0.6026	0.3131	0.1973	0.0929	0.0438	0.113	9.28	7
500	0	0.1	0.3	0.053	0.4806	–	–	–	–	6.727	37.84	8
500	0	1	0.3	0.28	0.0412	–	–	–	–	0.959	5.16	8
500	0	10	0.3	0.281	0.0393	–	–	–	–	0.101	5.13	8
500	2	0.1	0.3	0.05	0.5137	0.4926	0.1673	–	–	8.248	36.3	8
500	2	1	0.3	0.05	0.5956	0.4594	0.1537	–	–	1.139	32.71	8
500	2	10	0.3	0.05	0.6009	0.4581	0.1474	–	–	0.119	32.51	8
500	4	0.1	0.3	0.051	0.6018	0.5156	0.5771	0.2994	0.3613	8.768	44.47	8
500	4	1	0.3	0.051	0.6679	0.5149	0.5196	0.3133	0.2069	1.176	35.27	8
500	4	10	0.3	0.051	0.6782	0.5157	0.5026	0.321	0.1604	0.122	33.46	8
50	0	0.1	0.3	0.05	0.4806	–	–	–	–	6.435	37.84	9
50	0	1	0.3	0.248	0.109	–	–	–	–	0.93	6.34	9
50	0	10	0.3	0.268	0.0679	–	–	–	–	0.099	5.58	9
50	2	0.1	0.3	0.05	0.5283	0.4855	0.1835	–	–	7.642	35.84	9
50	2	1	0.3	0.05	0.6022	0.4571	0.1488	–	–	1.124	32.42	9
50	2	10	0.3	0.05	0.6141	0.4523	0.1513	–	–	0.118	32.1	9
50	4	0.1	0.3	0.051	0.5984	0.5045	0.5728	0.3266	0.3451	8.092	43.46	9
50	4	1	0.3	0.05	0.6778	0.5161	0.5139	0.3117	0.1878	1.159	34.52	9
50	4	10	0.3	0.051	0.6772	0.52	0.4944	0.3154	0.1592	0.122	32.83	9
500	2	0.1	0.299	0.091	0.4992	0.3986	0.0504	–	–	7.696	19.98	10
500	2	1	0.285	0.066	0.5991	0.3776	0.0498	–	–	1.121	19.99	10
500	2	10	0.287	0.067	0.6152	0.3743	0.0472	–	–	0.118	19.99	10
500	4	0.1	0.266	0.066	0.5887	0.3854	0.4719	0.2386	0.0855	7.995	19.97	10
500	4	1	0.277	0.059	0.6824	0.4487	0.4198	0.2382	0.0523	1.146	19.96	10
500	4	10	0.283	0.065	0.6865	0.4656	0.4074	0.2314	0.0479	0.12	19.99	10
500	2	0.1	0.335	0.085	0.5497	0.497	0.198	–	–	8.344	39.92	10
500	2	1	0.377	0.131	0.6082	0.4852	0.1923	–	–	1.145	39.92	10
500	2	10	0.347	0.094	0.62	0.4809	0.2022	–	–	0.119	39.86	10
500	4	0.1	0.304	0.054	0.6586	0.5083	0.551	0.3153	0.2875	8.719	39.81	10
500	4	1	0.311	0.053	0.6905	0.5325	0.5214	0.342	0.2255	1.183	39.65	10
500	4	10	0.312	0.054	0.6968	0.5355	0.5166	0.3405	0.2039	0.123	39.03	10

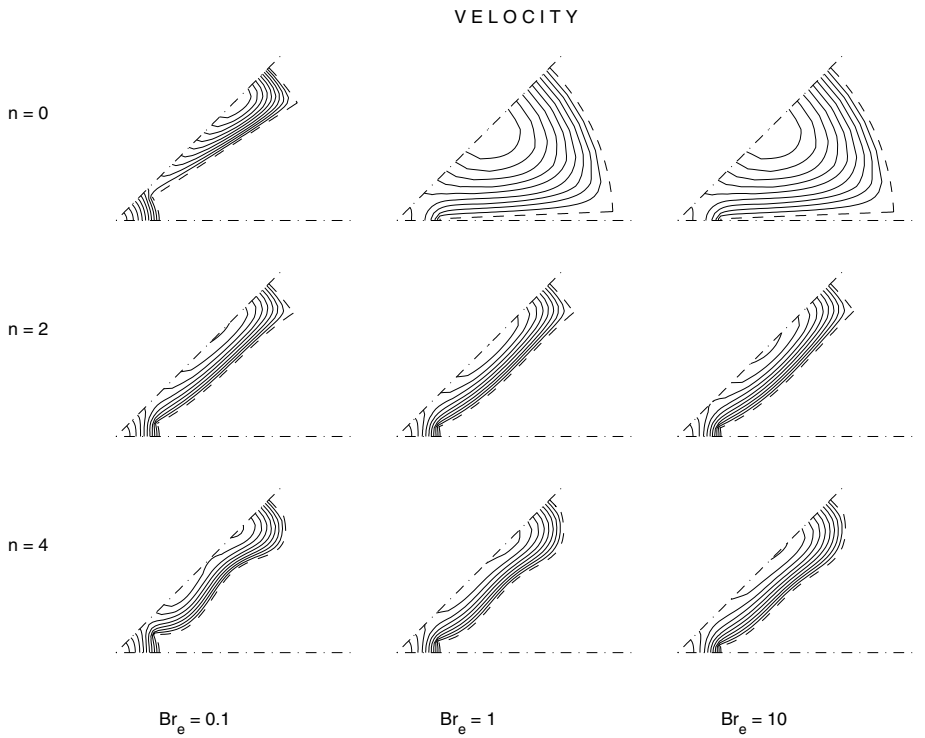

Fig. 3. Velocity distributions in the cross-section of the geometries of Fig. 2. Curves are drawn every 10% of the maximum velocity.

To consider different effects of viscous dissipation, an equivalent Brinkman number has been introduced:

$$Br_e = \frac{\mu \bar{u}}{2(R+s)q''} \tag{25}$$

where $\bar{u}$ is the average velocity. Such a parameter corresponds to the Brinkman number which would be calculated if the same coolant fluid flowed in a finnless tube with a zero wall thickness and radius equal to $R+s$. For the equivalent Brinkman number values ranging from 0.1 to 10 have been considered. In an optimized finned tube such as those obtained in Ref. [13], with an external radius equal to 0.01 m and an hydraulic diameter equal to 0.005 m, where a light oil flows at a Reynold number close to 2000, the equivalent Brinkman number is equal to 10 only when either the coolant temperature is moderate (15 °C for q'' equal to 15 W/m^2) or the transferred heat flux is low (q'' equal to 1 W/m^2 for T_b equal to 40 °C). Therefore, such a value of the equivalent Brinkman number can be considered as a limit for heat transfer problems of practical interest.

To the finite element model a grid of 16×52 elements (17×53 nodes) has been employed. More closed grids have been tested without finding any significant variation in Nu_e. In the testing cases, a grid of 20×52 elements produced alterations in Nu_e of less than 0.4%, and a grid of 16×65 elements caused changes of less than 0.2%. In the limit case of α equal to 0, the velocity and the temperature distributions obtainable with the model with the selected grid are in good agreement with the analytical one-dimensional solution and the numerical error on Nu_e is equal to 0.06%.

In the genetic algorithm populations of 20 samples and a selection percentage equal to 20 were established. During parameter reproduction, uniformly distributed between −10% and +10% random errors were introduced. The genetic algorithm was stopped after 50 generations from that time in which an improvement was no longer observed. As prototypes, finned tubes having σ equal to 0.1 and ϕ_i equal to $\beta/2$ were employed.

3.1. Optimization without constraints

In Fig. 2a some finned tube geometries which maximize Nu_e are shown for n equal to 0, 2 and 4, β equal to $\pi/4$ and γ equal to 500 in correspondence of three values of Br_e. The same conditions of the analysis neglecting viscous dissipation [13] have been imposed. Moreover, the range of Br_e corresponds to situations of practical interest for heat removing systems. The describing parameters of the optimum geometries are reported in Table 1 together with the average finned tube thickness, the equivalent Nusselt number, and the normalized

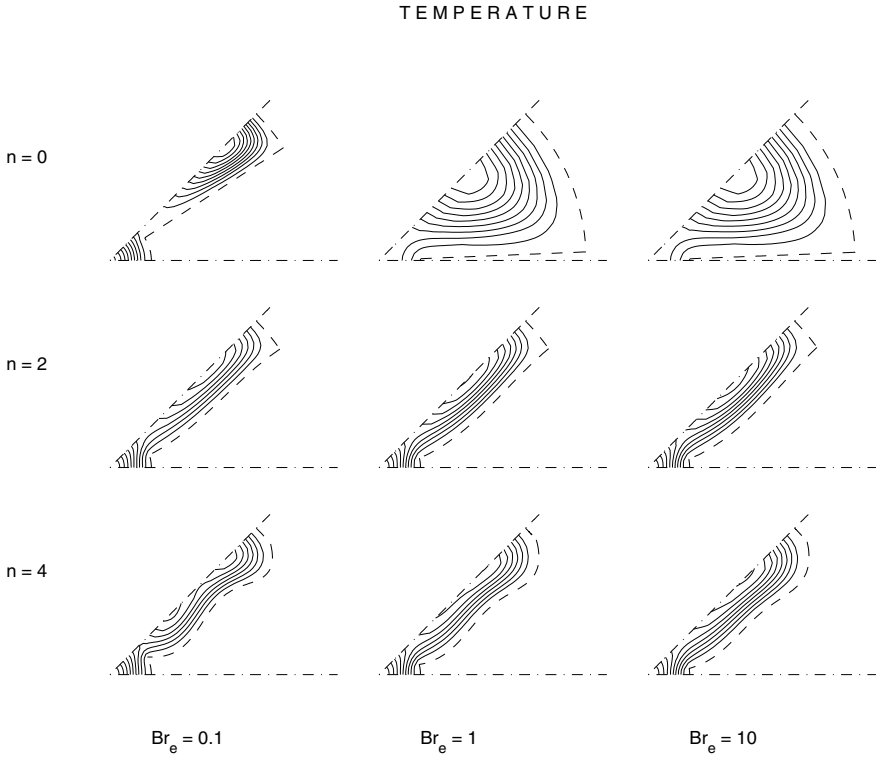

Fig. 4. Temperature distributions in the cross-section of the geometries of Fig. 4. Curves are drawn every 10% of the difference between the maximum and minimum temperatures.

hydraulic resistance. The table also contains the characteristic parameters of the optimum geometries which will be discussed in the following.

Fig. 2b shows the optimum finned tube geometries obtained in Ref. [13] under the same conditions of Fig. 2a by neglecting viscous dissipation. Comparing Fig. 2a with Fig. 2b, it is possible to observe that the effect of viscous dissipation noticeably modifies the optimum second and fourth order geometries, even when the equivalent Brinkman number is low ($Br_e = 0.1$). In particular, the optimum geometries obtained by taking viscous dissipation into account have fins with a flatter lateral profile, which induces lower velocity gradients and viscous dissipative phenomena. Moreover, by increasing Br_e, for every profile polynomial order, the channel cross-section becomes wider. This is particularly evident in case of zero order polynomial profiles.

The heat transfer effectiveness of the finned tubes is in fact improved by an increment in the convection coefficient. Such a parameter can be increased by narrowing the channel cross-section and inducing higher velocity and temperature gradient near the fin surface. When the viscosity or the velocity is high, or the imposed heat flux is low (Br_e is high) the viscous dissipative effect induced by high velocity gradients prevails on the influence of a high convection coefficient, resulting in a reduction of the heat transfer effectiveness of the finned tube. In this cases, the optimum geometries have a wider channel cross-section, which produces lower velocity and temperature gradients (Figs. 3 and 4).

Such a phenomenon can be better understood by observing the dependence of a simple fin profile tube geometry on the channel width in correspondence with different value of Br_e. In Fig. 5 the equivalent Nusselt number of a zero order fin profile tube geometry with an unfinned wall thickness constrained to 0.05 times the internal radius, under the same conditions of Fig. 2, is reported as a function of the profile angle (ϕ_0) in correspondence with three values of Br_e. When Br_e is equal to 0.1, the maximum in Nu_e comes from a compromise between the exigence of narrowing the channels between the fins in order to increase velocity and temperature gradients (to increase the convection coefficient) and that of enlarging the channels in order to make the velocity and temperature more uniform (to reduce the drop between the external surface and bulk temperature). When Br_e is higher, the effect of viscous dissipation increases and just a local maximum in Nu_e occurs in correspondence with that compromise. For this reason the thickness of zero order polynomial profile fins of Fig. 2 falls to

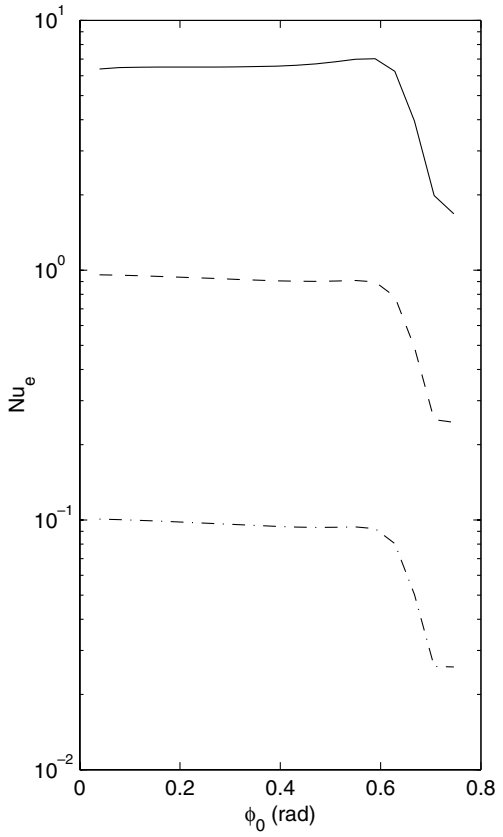

Fig. 5. Equivalent Nusselt number of a finned tube with zero order polynomial profile fins versus the profile angle for α equal to 0.8, β to $\pi/4$, γ to 500, σ to 0.05, and Br_e to 0.1 (continuous line), 1 (dashed line), and 10 (dot-dashed line).

very low values when Br_e is equal to 1 or 10. It must be noticed that in these cases, since the fin base is thin, the conductance of the tube wall is increased by enlarging the wall thickness. Such a phenomenon is less evident when Br_e is equal to 10, since the contribution of the heat flux imposed on the wall is less significant.

Referring to the optimum geometries of Fig. 2, it is important to observe that the effect of viscous dissipation, in general, reduces the equivalent Nusselt number and the improvements in the heat transfer of higher order polynomial profile fins. In particular, fourth order profile fins do not perform much better than second order ones. However, referring to the equivalent Nusselt number of zero order profile fins, increments from 18% to 21% are obtainable with second order profiles, and increments from 23% to 26% with fourth order profiles.

3.2. Constrained solid volume

It is also interesting to investigate how the effect of viscous dissipation modifies the optimum geometries when the available solid volume is limited. In Figs. 6–8 the geometries which maximize Nu_e when n is equal 0, 2, and 4 and $\overline{\sigma}$ is equal to 0.1, 0.2, and 0.3 in correspondence with three values of Br_e are shown. It is evident that the effect of viscous dissipation produces flatter fins and larger channels in the optimum geometries even when the solid volume of the finned tube is constrained. In particular, when the average wall thickness is constrained to 0.2, viscous dissipation produces large changes in the optimum geometries having fourth order profile fins. As a consequence, when Br_e is equal to 1 and 10, fourth order profile geometries are very similar to the second order ones, allowing very small improvements in Nu_e.

It must be noticed that the equivalent Nusselt number of zero order profile optimum geometries for a high value (1 or 10) of Br_e does not significantly change with the available solid volume, and, in particular, with the wall thickness. Since, on the contrary, the heat transfer effectiveness of higher order profile optimum geometries decrease with the available solid volume, the improvements in Nu_e provided by such geometries are very small when $\overline{\sigma}$ is low.

3.3. Reduced thermal conductivity in the solid

In Fig. 9 the optimum geometries obtained for n equal to 0, 2 and 4, σ constrained to 0.3 and γ equal to 50 are shown. It can be observed that these geometries are very similar to those obtained under the same conditions by assigning to γ a value which is higher for a magnitude order. Only in the situations where fins are very thin the reduction of the ratio between the thermal conductivity of the solid and that of the fluid produces evident differences.

3.4. Constrained hydraulic resistance

Lastly, it is interesting to investigate how the effect of viscous dissipation modifies the optimum geometries when the hydraulic resistance of the finned duct is limited. In Fig. 10 the geometries which maximize Nu_e when n is equal to 2 and 4 and ς is constrained to be no higher than 20 and 40 in correspondence with three values of Br_e are shown. Even in this case, a stronger effect of viscous dissipation causes flatter fin profile in the optimum geometries. However, since the constraint on ς requires larger channels the effect of viscous dissipation produces less noticeable modifications in the optimum geometries.

4. Conclusions

The results obtained demonstrate that the effect of viscous dissipation noticeably modifies the optimum

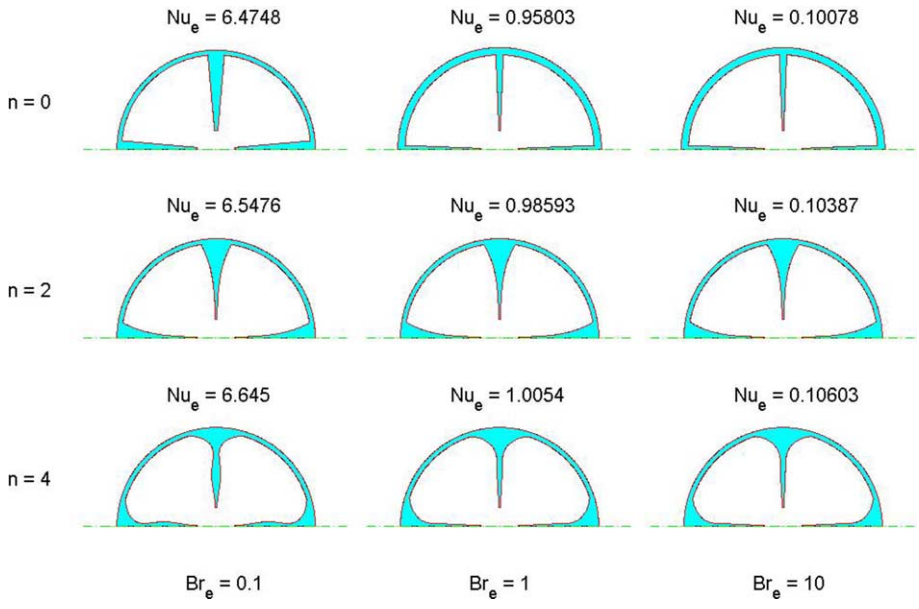

Fig. 6. Finned tube geometries which maximize Nu_e when α is equal to 0.8, β to $\pi/4$, γ to 500 and $\overline{\sigma}$ is constrained to 0.1.

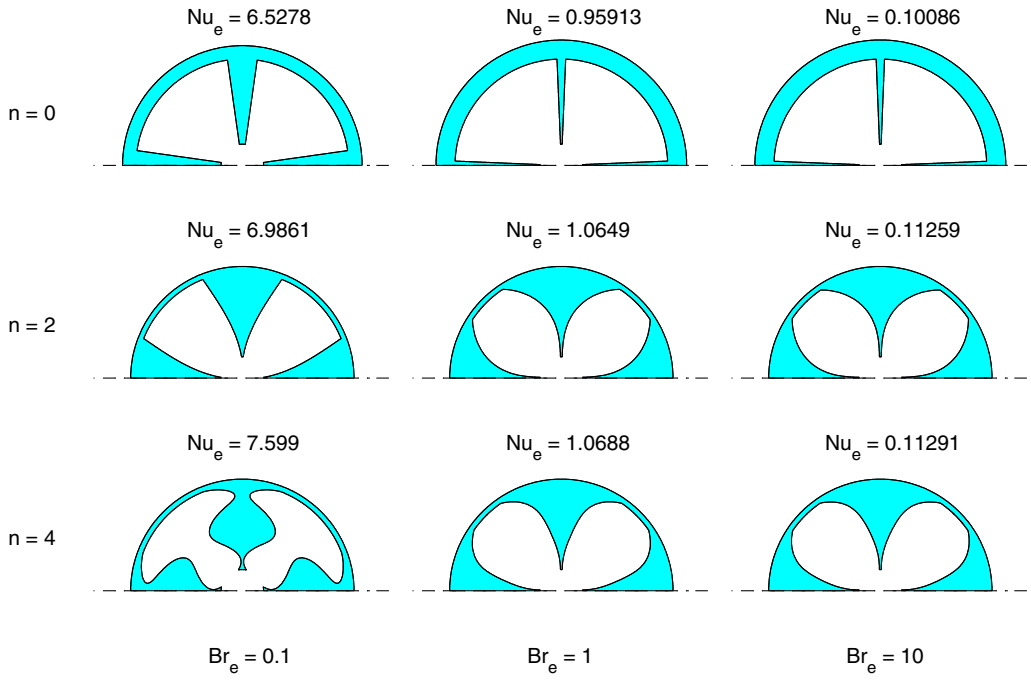

Fig. 7. Finned tube geometries which maximize Nu_e when α is equal to 0.8, β to $\pi/4$, γ to 500 and $\overline{\sigma}$ is constrained to 0.2.

geometry of a finned tube. The following conclusions are to be considered:

1. The finned tube geometries which provide the best heat transfer performance in presence of stronger effects of viscous dissipation have flatter fin profiles and wider channels between the fins than in case viscous dissipation is low.
2. The effect of viscous dissipation reduces the heat transfer effectiveness of the finned tube and the

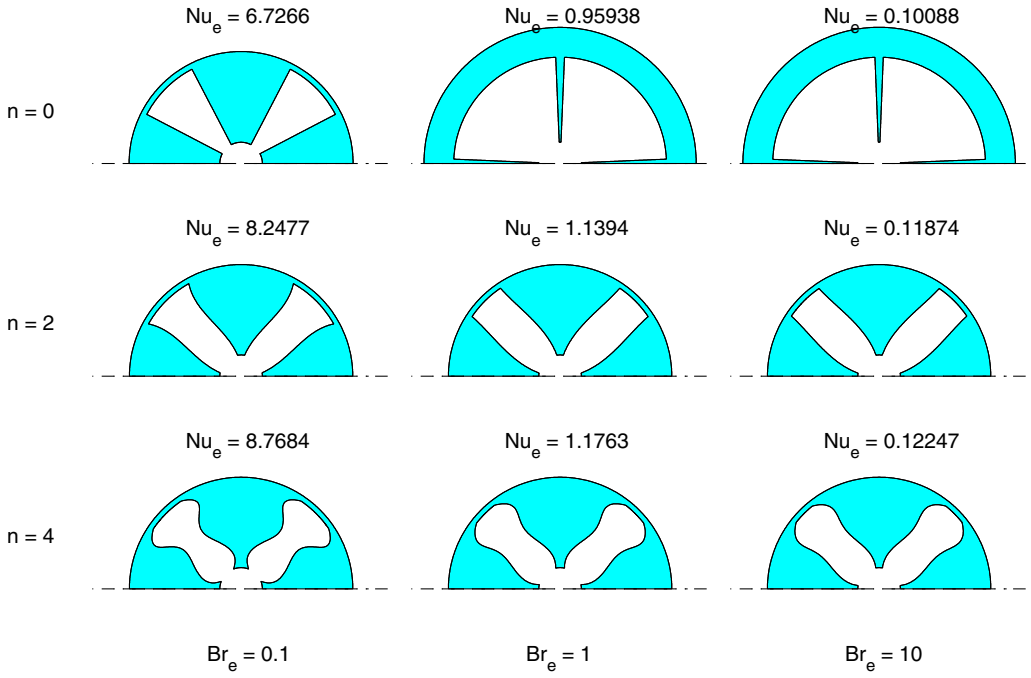

Fig. 8. Finned tube geometries which maximize Nu_e when α is equal to 0.8, β to $\pi/4$, γ to 500 and $\overline{\sigma}$ is constrained to 0.3.

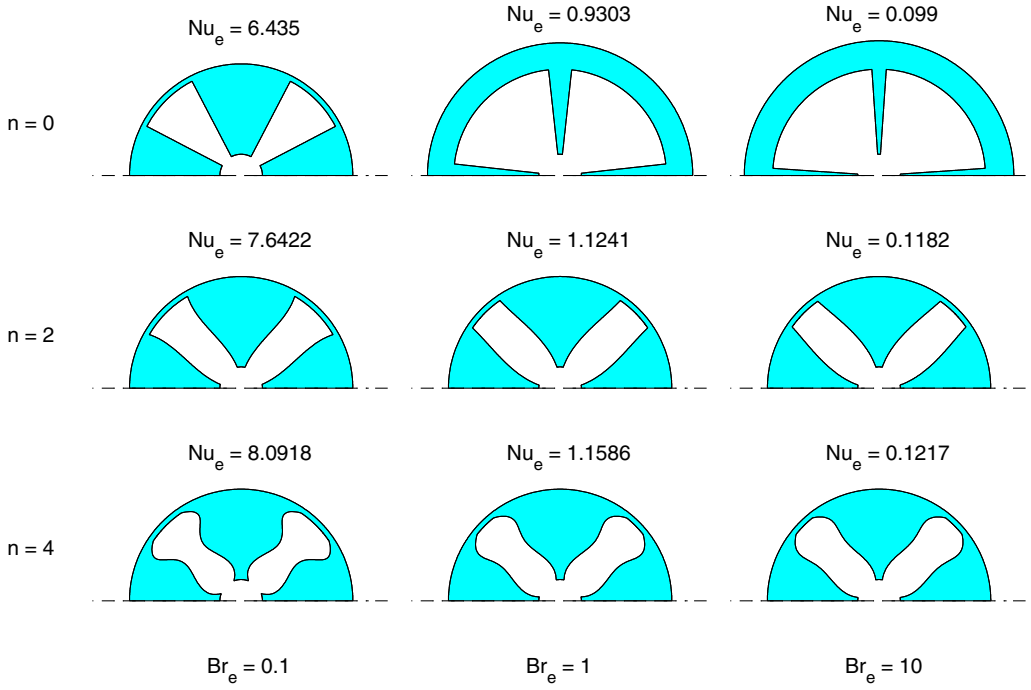

Fig. 9. Finned tube geometries which maximize Nu_e when α is equal to 0.8, β to $\pi/4$ and γ to 50.

improvements provided by geometries having higher order polynomial profile fin.

3. The effect of viscous dissipation causes evident changes in the optimum geometries and reductions

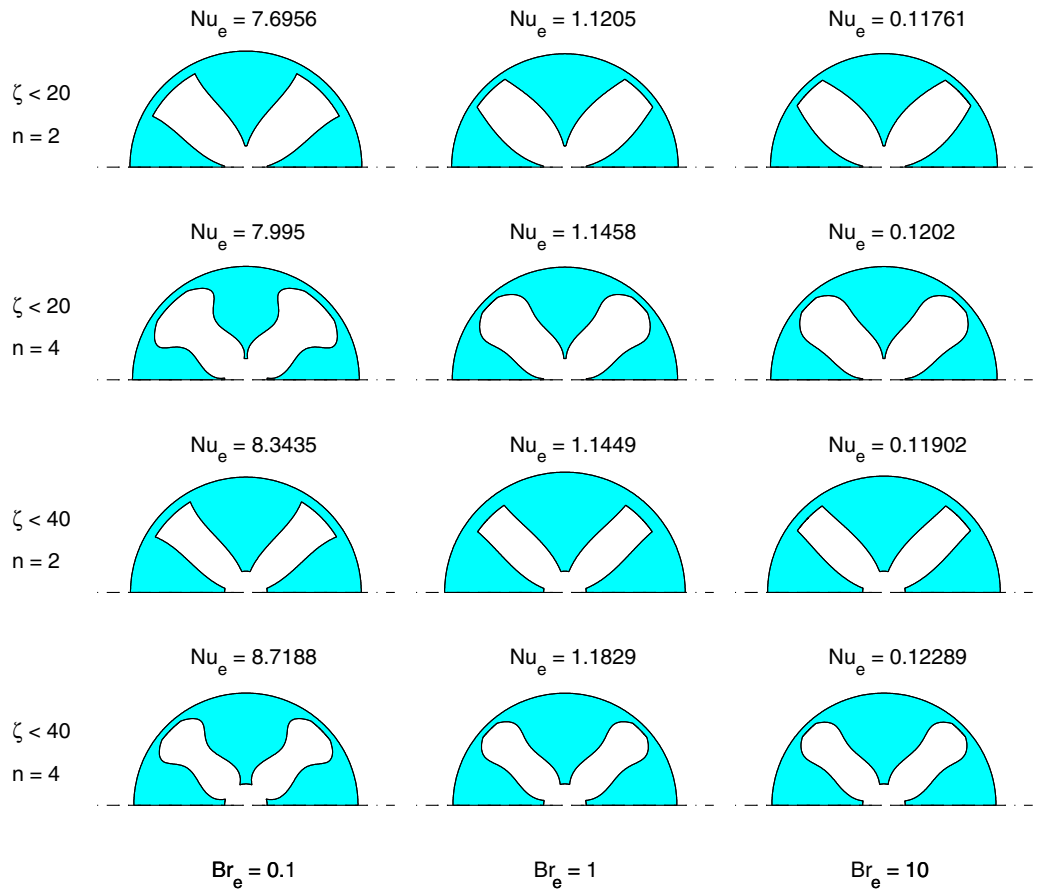

Fig. 10. Finned tube geometries which maximize Nu_e when α is equal to 0.8, β to $\pi/4$, γ to 500 and ς is constrained to be no more than 20 and 40.

in the heat transfer effectiveness even when the available solid volume is constrained.

4. When the hydraulic resistance is constrained, the differences between the optimum geometries obtained under different conditions of viscous dissipation are more limited.

It must be noticed that some parameters which determine the effect of viscous dissipation, under certain conditions, depend on the finned tube geometry. This is for example the case of the average coolant velocity, which depends on the finned tube cross-sectional area when the coolant flow rate is established or determined by constraints on the pressure drop and hydraulic resistance. Therefore, in some practical applications, it could be necessary to search the optimum finned tube geometry by considering more complex relationships between the parameters of the problem and more conditioning constraints than in the present analysis.

The present investigation has been limited to the case of laminar flow. Since the presence of eddies increases the apparent viscosity, in the case of turbulent flow the optimum finned tube geometries are expected to have even more flatter fin profiles and wider channels between the fins.

References

[1] H.C. Brinkman, Heat effects in capillary flow I, Appl. Sci. Res. A 2 (1951) 120–124.
[2] V.P. Tyagi, Laminar forced convection of a dissipative fluid in a channel, ASME J. Heat Transfer 88 (1966) 161–169.
[3] J.W. Ou, K.C. Cheng, Viscous dissipation effects on thermal entrance region heat transfer in pipes with uniform wall heat flux, Appl. Sci. Res. 28 (1973) 289–301.
[4] J.W. Ou, K.C. Cheng, Viscous dissipation effects on thermal entrance heat transfer in laminar and turbulent pipe flows with uniform wall temperature, ASME paper 74-HT-50, 1974.
[5] T.F. Lin, K.H. Hawks, W. Leidenfrost, Analysis of viscous dissipation effect on thermal entrance heat transfer in

laminar pipe flows with convective boundary conditions, Wärme und Stoffübertragung 17 (1983) 97–105.
[6] T. Basu, D.N. Roy, Laminar heat transfer in a tube with viscous dissipation, Int. J. Heat Mass Transfer 28 (1985) 699–701.
[7] R.K. Shah, M.S. Bhatti, Laminar convective heat transfer in ducts, in: S. Kakac, R.K. Shah, W. Aung (Eds.), Handbook of Single-phase Convective Heat Transfer, Wiley, New York, 1987, pp. 3–12.
[8] A. Lawal, A.S. Mujumdar, The effect of viscous dissipation on heat transfer to power law fluids in arbitrary cross-sectional ducts, Wärme und Stoffübertragung 27 (1992) 437–446.
[9] A. Barletta, On forced convection in a circular duct with slug flow and viscous dissipation, Int. Commun. Heat Mass Transfer 23 (1996) 69–78.
[10] E. Zanchini, Effect of viscous dissipation on the asymptotic behaviour of laminar forced convection in circular tubes, Int. J. Heat Mass Transfer 40 (1997) 169–178.
[11] A. Barletta, E. Zanchini, Forced convection in the thermal entrance region of a circular duct with slug flow and viscous dissipation, Int. J. Heat Mass Transfer 40 (1997) 1181–1190.
[12] G.L. Morini, M. Spiga, P. Tartarini, Laminar viscous dissipation in rectangular ducts, Int. Commun. Heat Mass Transfer 25 (1996) 551–560.
[13] G. Fabbri, Heat transfer optimization in internally finned tubes under laminar flow conditions, Int. J. Heat Mass Transfer 41 (10) (1998) 1243–1253.
[14] N. Queipo, R. Devarakonda, J.A.C. Humphrey, Genetic algorithms for thermosciences research: application to the optimized cooling of electronic components, Int. J. Heat Mass Transfer 37 (6) (1994) 893–908.
[15] G. Fabbri, A genetic algorithm for fin profile optimization, Int. J. Heat Mass Transfer 40 (9) (1997) 2165–2172.
[16] G. Fabbri, Optimum profiles for asymmetrical longitudinal fins in cylindrical ducts, Int. J. Heat Mass Transfer 42 (3) (1999) 511–523.
[17] G. Fabbri, Heat transfer optimization in corrugated wall channels, Int. J. Heat Mass Transfer 43 (2000) 4299–4310.
[18] J. Parker, J. Boggs, E. Blick, Introduction to Fluid Mechanics and Heat Transfer, Addison-Wesley, 1969 (Chapter 4).